



HHS Public Access

Author manuscript

J Autism Dev Disord. Author manuscript; available in PMC 2016 September 06.

Published in final edited form as:

J Autism Dev Disord. 2015 February ; 45(2): 395–405. doi:10.1007/s10803-013-1904-x.

Neuromagnetic Oscillations Predict Evoked-Response Latency Delays and Core Language Deficits in Autism Spectrum Disorders

J. Christopher Edgar,

Department of Radiology, Lurie Family Foundations MEG Imaging Center, The Children's Hospital of Philadelphia, Wood Bldg, Suite 2115, 34th St. and Civic Center Blvd, Philadelphia, PA 19104, USA

Sarah Y. Khan,

Department of Radiology, Lurie Family Foundations MEG Imaging Center, The Children's Hospital of Philadelphia, Wood Bldg, Suite 2115, 34th St. and Civic Center Blvd, Philadelphia, PA 19104, USA

Lisa Blaskey,

Department of Radiology, Lurie Family Foundations MEG Imaging Center, The Children's Hospital of Philadelphia, Wood Bldg, Suite 2115, 34th St. and Civic Center Blvd, Philadelphia, PA 19104, USA

Department of Pediatrics, The Children's Hospital of Philadelphia, Philadelphia, PA, USA

Vivian Y. Chow,

Department of Radiology, Lurie Family Foundations MEG Imaging Center, The Children's Hospital of Philadelphia, Wood Bldg, Suite 2115, 34th St. and Civic Center Blvd, Philadelphia, PA 19104, USA

Michael Rey,

Department of Radiology, Lurie Family Foundations MEG Imaging Center, The Children's Hospital of Philadelphia, Wood Bldg, Suite 2115, 34th St. and Civic Center Blvd, Philadelphia, PA 19104, USA

William Gaetz,

Department of Radiology, Lurie Family Foundations MEG Imaging Center, The Children's Hospital of Philadelphia, Wood Bldg, Suite 2115, 34th St. and Civic Center Blvd, Philadelphia, PA 19104, USA

Katelyn M. Cannon,

Department of Radiology, Lurie Family Foundations MEG Imaging Center, The Children's Hospital of Philadelphia, Wood Bldg, Suite 2115, 34th St. and Civic Center Blvd, Philadelphia, PA 19104, USA

edgarj@email.chop.edu.

Electronic supplementary material The online version of this article (doi:10.1007/s10803-013-1904-x) contains supplementary material, which is available to authorized users.

Conflict of interest No author declares a conflict of interest.

Justin F. Monroe,

Department of Radiology, Lurie Family Foundations MEG Imaging Center, The Children's Hospital of Philadelphia, Wood Bldg, Suite 2115, 34th St. and Civic Center Blvd, Philadelphia, PA 19104, USA

Lauren Cornew,

Department of Radiology, Lurie Family Foundations MEG Imaging Center, The Children's Hospital of Philadelphia, Wood Bldg, Suite 2115, 34th St. and Civic Center Blvd, Philadelphia, PA 19104, USA

Saba Qasmieh,

Department of Pediatrics, The Children's Hospital of Philadelphia, Philadelphia, PA, USA

Song Liu,

Department of Radiology, Lurie Family Foundations MEG Imaging Center, The Children's Hospital of Philadelphia, Wood Bldg, Suite 2115, 34th St. and Civic Center Blvd, Philadelphia, PA 19104, USA

John P. Welsh,

Center for Integrative Brain Research, Seattle Children's Research Institute, Seattle, WA, USA

Susan E. Levy, and

Department of Pediatrics, The Children's Hospital of Philadelphia, Philadelphia, PA, USA

Timothy P. L. Roberts

Department of Radiology, Lurie Family Foundations MEG Imaging Center, The Children's Hospital of Philadelphia, Wood Bldg, Suite 2115, 34th St. and Civic Center Blvd, Philadelphia, PA 19104, USA

Abstract

Previous studies have observed evoked response latency as well as gamma band superior temporal gyrus (STG) auditory abnormalities in individuals with autism spectrum disorders (ASD). A limitation of these studies is that associations between these two abnormalities, as well as the full extent of oscillatory phenomena in ASD in terms of frequency and time, have not been examined. Subjects were presented pure tones at 200, 300, 500, and 1,000 Hz while magnetoencephalography assessed activity in STG auditory areas in a sample of 105 children with ASD and 36 typically developing controls (TD). Findings revealed a profile such that auditory STG processes in ASD were characterized by pre-stimulus abnormalities across multiple frequencies, then early high-frequency abnormalities followed by low-frequency abnormalities. Increased pre-stimulus activity was a 'core' abnormality, with pre-stimulus activity predicting post-stimulus neural abnormalities, group membership, and clinical symptoms (CELF-4 Core Language Index). Deficits in synaptic integration in the auditory cortex are associated with oscillatory abnormalities in ASD as well as patient symptoms. Increased pre-stimulus activity in ASD likely demonstrates a fundamental signal-to-noise deficit in individuals with ASD, with elevations in oscillatory activity suggesting an inability to maintain an appropriate 'neural tone' and an inability to rapidly return to a resting state prior to the next stimulus.

Keywords

Auditory; Autism spectrum disorders; M100; Gamma; Evoked; Inter-trial coherence; Phase-locking; Magnetoencephalography

Superior Temporal Gyrus Spectro-temporal Abnormalities in Autism Spectrum Disorders

Magnetoencephalography (MEG) studies examining superior temporal gyrus (STG) auditory activity in individuals with Autism Spectrum Disorders (ASD) almost uniformly report abnormalities. For example, in the time-domain, several studies have reported delays in the latency of auditory-evoked response peaks in autism, especially the 100 ms (M100) STG auditory response (Gage et al. 2003; Roberts et al. 2010). Although delayed responses have been hypothesized to contribute to language deficits in ASD (Oram Cardy 2008; Roberts et al. 2008), there is not clear mechanistic support for such a relationship. Emerging evidence also suggests impairments in auditory oscillatory activity in ASD. Presenting 40 Hz click trains to children with autism and age-matched controls, Wilson et al. (Wilson et al. 2007) observed decreased left-hemisphere 40 Hz steady-state gamma band activity in autism. Presenting 1,000 Hz tones and examining the early STG transient gamma-band response, Rojas et al. (Rojas et al. 2008) observed decreased left and right 40 Hz inter-trial coherence (ITC, also called phase-locking factor) in adults with autism as well as in the parents of children with autism, leading Rojas et al. to argue for a deficit in autism in the ability to time gamma oscillations to external stimuli.

It is unknown whether a delayed M100 response and decreased auditory gamma activity reflect a single abnormality or if the two abnormalities are distinct. In addition, previous auditory time–frequency studies have focused exclusively on gamma-range activity (~30–50 Hz). The motivation for this is likely due to (1) the association between inhibitory interneuron processes and gamma activity (e.g., see Bibbig et al. 2002; Whittington et al. 2000), and (2) a hypothesized inhibitory interneuron dysfunction in ASD (e.g., Casanova et al. 2002; Uhlhaas and Singer 2007). High frequency activity, however, is not the only, or even the primary, component of auditory evoked responses, and many studies show a coupling of low- and high-frequency activity such that high-frequency abnormalities are likely associated with low-frequency abnormalities (e.g., see Canolty and Knight 2010; Lakatos et al. 2004). Studies observing low-frequency resting-state abnormalities in ASD also indicate the need to assess oscillatory processes pre- and post-stimulus across a broad range of frequencies in order to fully characterize neural abnormalities in ASD (e.g., see Cantor et al. 1986; Murias et al. 2007; Cornew et al. 2012).

In the present study, source-localized STG time-domain and time–frequency activity (evoked and ITC) to transient sinusoidal tones was examined in a large sample of children with ASD and age-matched TD controls. The following hypotheses were tested: (1) Replicating previous findings from a smaller but overlapping group of subjects (Roberts et al. 2010), children with ASD would show delayed right-hemisphere M100 STG responses. (2) Based on previous gamma findings (Wilson et al. 2007; Rojas et al. 2008), children with ASD

would show decreased early evoked gamma activity and ITC. (3) Post-stimulus gamma band and M100 latency abnormalities would be related, with decreased early evoked gamma activity predicting later M100 responses. (4) Pre-stimulus and post-stimulus oscillatory abnormalities other than gamma-band abnormalities would be observed. (5) Finally, as some studies suggest a relationship between impaired auditory processing and language abilities (Oram Cardy 2008; Roberts et al. 2011), STG abnormalities were predicted to be related to performance on a test of language ability. As Roberts et al. (2010) also observed associations between STG auditory measures and age, to assess changes in these measures across development, associations between age and STG M100 latency and time–frequency measures were examined.

Methods

Participants

Recruitment procedures and inclusion/exclusion information are detailed in Roberts et al. (2010) (see also online supplement). Although individuals with ASD were not screened for co-morbid disorders (e.g., ADHD), individuals with known neurological or genetic conditions (e.g., seizure disorder, head injury, Fragile X) or mental retardation (Nonverbal and Verbal IQ both below 75) were excluded. Data were analyzed from 105 children with ASD (11 Female) and 36 TD (19 females) children. In the children with ASD, mean score on the Autism Diagnostic Observation Schedule was 12.5 (SD = 4.44; module 3 administered in nearly all cases), mean score on the Social Responsiveness Scale was 81.73 (SD = 20.27), and mean score on the Social Communication Questionnaire was 20.77 (SD = 9.49).

The age range of both groups was 6–16 years, and t-tests demonstrated that the groups were similar in age [TD = 10.90 years \pm 2.78; ASD = 10.07 years \pm 2.37; $t(139) = 1.74$, *ns*]. Groups did not differ on their *Wechsler Intelligence Scale for Children–IV* Perceptual Reasoning Index scores [TD = 108.83 \pm 14.64; ASD = 103.61 \pm 15.18; $t(139) = 1.80$, *ns*]. Individuals with ASD had lower CELF-4 Core Language Index scores [TD = 109.44 \pm 11.29; ASD = 88.70 \pm 19.37; $t(139) = 6.08$, $p < 0.01$]. Additional demographic information is provided in the online supplement.

Auditory Stimuli

Auditory stimuli were delivered via eartip inserts (Etymotic ER3A, Elk Grove, IL). Children with ASD tended to have weaker hearing (detection thresholds \sim 5 dB higher than the TD group), and the TD and ASD groups differed in hearing thresholds in the left, $t(137) = 1.94$, $p < 0.05$, and right ear, $t(137) = 2.88$, $p < 0.01$ (two participants were missing threshold information). Stimuli, however, were presented 45 dB above individually-determined thresholds, controlling for individual (and group) hearing threshold differences. During the MEG exam, 200, 300, 500 and 1,000 Hz sinusoidal tones of 300 ms duration (with 10 ms onset-offset ramps) were presented binaurally. Tones were randomly presented, with a 1 s interstimulus interval (jittered \pm 100 ms). Over approximately 7 min of recording time, 105 tones at each of the 4 frequencies were presented.

MEG Recordings

Recordings were obtained using a 275-channel MEG system (VSM MedTech Inc., Coquitlam, BC). Three head-position indicator coils attached to the scalp provided continuous specification of the position and orientation of the MEG sensors relative to the head. To minimize fatigue, subjects viewed (but did not listen to) a movie projected onto a screen positioned at a comfortable viewing distance. To aid in the identification of eye-blink activity, the electro-oculogram (EOG; bipolar oblique, upper right and lower left sites) was collected. Electrodes were also attached above the left and right collar bone for electro-cardiogram (ECG) recording. After a band-pass filter (0.03–300 Hz), EOG, ECG, and MEG signals were digitized at 1,200 Hz, with 3rd order gradiometer environmental noise reduction for the MEG data.

MEG Data Analysis

Epochs (500 ms pre-stimulus to 500 ms post-stimulus) were defined from the continuous recording. Eye-blink and heartbeat activity were corrected using procedures outlined in Roberts et al. (2010) (see supplement). Epochs with artifacts other than blinks or heartbeat were rejected by amplitude and gradient criteria (amplitude >1,200 fT/cm, gradients >800 fT/cm/sample). Non-contaminated epochs were averaged according to stimulus type.

Determination of the strength and latency of M100 sources in the left and right STG was accomplished by applying a standard source model to transform each individual's raw MEG surface activity into brain space [MEG data co-registered to the Montreal Neurological Institute (MNI) averaged brain] using a model with multiple sources (Scherg 1990; Scherg and Berg 1996; Scherg and von Cramon 1985). The source model was constructed by including (1) left and right STG dipole sources, and (2) nine fixed regional sources that model brain background activity and serve as probe sources for additional oscillatory activity. The eye-blink source vector derived for each participant was also included to remove eye-blink activity (Berg and Scherg 1994; Lins et al. 1993). The final source model serves as a source montage for the raw MEG (Scherg and Ebersole 1994; Scherg et al. 2002). Although the strength and latency of the M100 STG responses were obtained using a dipole source placed at a standard location, in each subject left and right hemisphere dipoles were oriented at the maximum of the M100. As such, although position was fixed, orientation of the standard STG sources was optimized for each subject. To measure M100 STG latency, a 1 Hz (6 dB/octave, forward) to 40 Hz (48 dB/octave, zero-phase) bandpass filter was applied and left and right M100 STG peak latency (measured in nano-Amperemeters, nAm) was calculated from the largest point in the M100 scoring window (90–190 ms) using in-house Mat-Lab software.

The calculation of single-trial phase and magnitude for the left and right STG sources used a modification of Hoehstetter et al. (2004) procedures where in each participant the derived source model was applied to the raw unfiltered data. Transformation from the time domain to the time–frequency domain used complex demodulation procedures (Papp and Ktonas 1977) implemented in BESA 5.2, using frequencies between 4 and 80 Hz, in steps of 2 Hz.¹ Continuous data were analyzed relative to the tone onset every 25 ms, utilizing ± 39.4 ms and

± 2.83 Hz (full width at half maximum parameters) of contiguous data at each 25 ms step. Time–frequency measures were computed from -400 to 400 ms relative to stimulus onset.

For evoked activity, background activity at each frequency (average power -400 to -100 ms) was calculated and subtracted as a function of frequency. In addition to evoked activity, for each time–frequency bin, a measure of phase-locking referred to as inter-trial coherence was

computed as $abs\left(\frac{1}{N}\sum_{k=1}^N e^{i\phi(k)}\right)$ where the sum is over all N trials, and $\phi(k)$ is the phase of the signal in the k th trial. Inter-trial coherence (ITC) is a normalized measure with $ITC = 1$ reflecting no phase variability and $ITC = 0$ reflecting maximal phase variability across trials (Lachaux et al. 1999).

Group Comparisons

For the time-domain analyses, unpaired t-tests probed group differences in M100 source strength and latency. Primary time–frequency analyses used t-tests to examine activity at each even-number frequency between 4 and 80 Hz in 25 ms bins and from 0 to 400 ms following stimulus onset, resulting in 624 t-tests (39 frequencies \times 16 time bins) for each hemisphere. To control family-wise error, a clustering method (which computes the probability of a random field of noise producing a cluster of a given size after the noise is thresholded at a given probability level) was used to obtain a corrected p value. The cluster size needed to obtain the desired familywise correction was determined using a standard fMRI package (AFNI Alpha-Sim, B. Douglas Ward), and clustering was performed with custom MatLab software. Using time (x axis) and frequency (y axis) full width at half maximum parameters that characterized the time–frequency filters (i.e., time = ± 39.4 ms and frequency = ± 2.83 Hz), an initial p value threshold of 0.05 for each time–frequency value and a cluster size threshold of 12 values (adjacent in time and/or frequency) provided a family-wise corrected $p = 0.05$.

Given differences in the percentage of males and females in each group, time–frequency analyses were re-run removing females (there were not enough females in the ASD group to compute female-only analyses). In addition, given the large age range (6–16 years), where time–frequency group differences were observed, region-of-interest analyses were run with age as a covariate to determine if the group differences remained after controlling for age (given that groups did not differ on age, the use of age as a covariate was appropriate).

Associations between each of the time–frequency measures and symptom severity were examined using the CELF-4 Core Language Index as well as the general ability index (GAI) IQ measure obtained from the *Wechsler Intelligence Scale for Children-IV* (WISC-IV; Wechsler 2003). The GAI provides an index of IQ without the confound of working memory and processing speed. Finally, correlations were also used to examine associations with age. As with the group comparisons, random field clustering controlled family-wise error in all correlation analyses.

¹Complex demodulation uses a finite impulse response (FIR) low-pass filter with a Gaussian wave shape in the time domain. Complex demodulation is equivalent to a wavelet transformation using Morlet-type wavelets with a fixed time–frequency resolution across frequencies.

Results

STG Latency

M100—Replicating findings reported in [Roberts et al. (2010); M100 latency data from approximately 50 % of the TD subjects and 25 % of the ASD subjects in the present study were reported in Roberts et al.], and supporting Hypothesis 1, group latency differences were observed only in the right hemisphere. The right-hemisphere M100 response peaked later in ASD than TD at 300 Hz [$t(119) = 1.57, p = 0.12$; marginally significant] and 500 Hz [$t(127) = 2.49, p = 0.01$], with an 7 and ~10 ms delay in the children with ASD for the right hemisphere response to 300 and 500 Hz tone stimuli, respectively.

STG Time–Frequency Activity

Evoked Oscillatory Activity—As shown in Fig. 1 and supporting Hypothesis 2, corrected clusters indicated a smaller increase in gamma evoked activity from ~50 to ~150 ms in the ASD than TD group (blue clusters). Gamma group differences were observed bilaterally and for all stimuli, although most prominent for 200, 300 and 500 Hz stimuli. Low-frequency evoked group differences were observed only in the right hemisphere at 500 Hz, the hemisphere and stimulus frequency where M100 group latency differences were most prominent.

Evoked time–frequency analyses were re-run including only males. Except for right 500 Hz where gamma group differences were marginally significant, the pattern of findings was unchanged. Examining ROIs where group differences were observed and re-running analyses with age as a covariate (full sample), the pattern of findings was unchanged.

Inter-trial Coherence (ITC)—As shown in Fig. 2 and supporting Hypothesis 2, corrected clusters indicated decreased left- and right-hemisphere gamma ITC in the ASD versus the TD group from ~50 to ~200 ms (blue clusters) at 300, 500, and 1,000 Hz (although the grand average plots suggest right gamma group differences at 200 Hz, this did not reach significance in this sample). ITC measures were more sensitive to low-frequency group differences than evoked measures. In particular, and supporting Hypothesis 3, decreased low-frequency ITC in the ASD than TD group was observed from 50 ms onwards at all frequencies except 1,000 Hz.

Inter-trial coherence time–frequency analyses were re-run including only males. The pattern of findings was unchanged for left 300 Hz and marginally significant for right 300 Hz. Excluding males, no group differences were resolved for left or right 500 Hz gamma activity. Examining ROIs where group differences were observed and re-running analyses with age as a covariate (full sample), the pattern of findings was unchanged.

Pre-stimulus Oscillatory Activity—Given that the four tones (i.e., 200, 300, 500, and 1,000 Hz) were randomly presented, group pre-stimulus differences were assessed after averaging the trials for all tones (approximately 420 trials). The pre-stimulus measure was computed by time–frequency transforming each trial and then averaging (i.e., a pre-stimulus total power measure was computed). Table 1 shows that except for right STG high gamma,

group differences were observed at all examined frequencies (i.e., theta, alpha, beta, low gamma, high gamma), with pre-stimulus power elevated in ASD.

Examining only males, the pattern of findings was unchanged for all pre-stimulus group comparisons. Re-running the analyses with age as a covariate (full sample), except for the right low and high gamma group comparisons becoming non-significant after removing variance associated with age, the pattern of findings was unchanged for all other pre-stimulus group comparisons.

Predicting Right M100 STG latency

To determine if time–frequency measures predicted right-hemisphere M100 STG latency and thus might account for the ASD latency delay, correlations indexed associations between M100 latency and pre-stimulus activity as well as post-stimulus activity preceding the M100 response. Greater left and right STG pre-stimulus activity (4–80 Hz) was associated with a longer M100 latency, with focused analyses showing that this association was generally observed across all frequency bands in both hemispheres. No post-stimulus time–frequency measure prior to M100 was associated with right M100 latency. As such, Hypothesis 3 with specificity for gamma band was not fully supported, although the functional significance of pre-stimulus electrophysiological anomaly is implicated.

To further examine associations between pre-stimulus activity, Group, and M100 latency, a hierarchical regression was performed with 4–80 Hz pre-stimulus activity entered first (given pre-stimulus group differences at most frequencies a single measure was computed), group second, and their interaction last, with M100 latency as the dependent variable. Regressions were conducted only where group latency differences were observed: right hemisphere response to 500 Hz tones. Added first, pre-stimulus activity accounted for significant variance ($r^2 = 0.07$, $p < 0.01$). Added second, Group account for significant additional variance ($r^2 = 0.02$, $p < 0.05$), indicating that both pre-stimulus activity and Group predicted unique variance in M100 latency. The interaction term was not significant.

Associations with Clinical Measures

Correlations indexed associations between time–frequency measures (i.e., evoked, ITC, and pre-stimulus activity) and CELF-4 Core Language Index and GAI scores in ASD.

Examining the family-wise corrected correlation maps, only associations with gamma activity were observed. In the left hemisphere, lower CELF-4 Core Language Index scores were associated with increased early 100 Hz post-stimulus evoked gamma ($r = 0.33$, $p < 0.001$; similar relationships not observed for any other frequency in either hemisphere). As shown in Fig. 3, there was a relationship between poorer performance on the CELF-4 Core Language Index and increased 30–50 Hz right-hemisphere pre-stimulus activity ($r = 0.36$, $p = 0.01$). No associations with GAI scores were observed.

Associations with Age

In Roberts et al. (2010), a relationship between age and M100 latency was observed. In the present study, zero-order correlations showed that age predicted M100 latency for all tones

($r_s > 0.40$, $p_s < 0.003$). As shown in Fig. 4, a strong association between age and pre-stimulus activity (average across tones) also was observed.

To examine the extent to which age accounts for M100 latency and pre-stimulus group differences, hierarchical regressions were performed with Age entered first, Group second, and their interaction last, with M100 STG latency or right STG pre-stimulus activity (4–80 Hz) as the dependent variable. With M100 latency as the dependent variable, the full regression model (Age, Group, interaction) accounted for significant variance in M100 latency ($p_s < 0.01$). For all analyses (i.e., each hemisphere and each tone), added first, Age accounted for significant variance ($p_s < 0.001$). Neither the Group nor the interaction term accounted for additional variance (Group marginally significant for right-hemisphere response to 500 Hz stimulus, $p = 0.08$).

With the pre-stimulus activity as the dependent variable, the full regression model (Age, Group, interaction) accounted for significant variance in pre-stimulus activity ($p_s < 0.001$). Added first, Age accounted for significant variance (left hemisphere = 28 %, $p < 0.001$; right hemisphere = 22 %, $p < 0.001$). Group accounted for additional variance only in the left hemisphere (5 %, $p < 0.003$). The interaction terms were not significant.

Discussion

In this study of 141 children, supporting Hypothesis 1, right-hemisphere M100 STG 500 Hz responses were approximately 10 ms delayed in ASD. Supporting Hypothesis 2 and replicating previous findings (Wilson et al. 2007; Rojas et al. 2008), decreased post-stimulus STG ~40 Hz evoked activity and ITC was observed bilaterally in children with ASD. As the above latency and gamma abnormalities were unrelated, Hypothesis 3 was not supported, indicating that these two abnormalities are somewhat distinct (e.g., gamma but not M100 latency group differences in the left hemisphere). Supporting Hypothesis 4, oscillatory abnormalities other than post-stimulus gamma abnormalities were observed in ASD. In particular, in addition to pre-stimulus abnormalities, evoked and ITC low-frequency (below ~20 Hz) group differences were observed.

The most striking finding in the present study was the pre-stimulus group difference (left and right hemisphere, 4–80 Hz). In addition to robustly differentiating groups, increased pre-stimulus activity predicted M100 latencies in both groups. Other findings also pointed to pre-stimulus activity as a measure warranting additional study: (1) higher 30–50 Hz right-hemisphere pre-stimulus activity (total power) was associated with lower CELF-4 Core Language Index scores, and (2) although age was associated with pre-stimulus measures, group differences in left hemisphere pre-stimulus activity (4–80 Hz) remained even after removing variance in pre-stimulus activity associated with age.

Greater pre-stimulus activity in ASD than TD likely indicates a fundamental neuronal signal-to-noise deficit in individuals with ASD. In particular, elevations in oscillatory activity observed in the present study across a broad range of frequencies (and also observed in resting state studies; e.g., see (Cantor et al. 1986; Murias et al. 2007; Cornew et al. 2012)) suggest an inability to maintain an appropriate ‘neural tone’ and perhaps also an inability to

rapidly return to a resting state prior to the next stimulus. Multiple factors likely account for the elevated background activity in ASD. For example, considering gamma activity, several studies have demonstrated that NMDAR antagonists (including ketamine, MK-801, and PCP) produce a dose-dependent increase in baseline gamma power using in vivo LFP and EEG recordings in awake rodents (Ehrlichman et al. 2009; Hakami et al. 2009; Lazarewicz et al. 2010; Leung 1985; Ma and Leung 2000, 2007; Pinault 2008; Saunders et al. 2012). The increase in gamma power associated with NMDAR antagonists is likely associated with reduced GABA release onto pyramidal neurons, as a number of studies have demonstrated dysfunction of interneurons and elevated pyramidal cell activity following NMDAR blockade or knockout mice (Belforte et al. 2010; Jackson et al. 2004; Santana et al. 2011; Saunders et al.).

In line with this hypothesis, it has recently been shown that fast-spiking interneurons expressing the calcium binding protein parvalbumin and acting through ionotropic GABA(A)-receptors are both necessary and sufficient to generate stimulus-evoked gamma-synchrony in vivo (Sohal et al. 2009; Cardin et al. 2009). In ASD, a growing body of research has shown GABA receptors to be downregulated in ASD (Fatemi et al. 2009), and ASD participants have shown decreased gamma-band oscillatory activity compared to controls (Wilson et al. 2007; Rojas et al. 2008; Orekhova et al. 2007). Interneurons defined by the fast-spiking phenotype and expression of the calcium-binding protein parvalbumin have been implicated in gamma oscillations (e.g., (Tamas et al. 2000; Whittington et al. 1995), and in vivo mouse studies show that inhibiting parvalbumin interneurons suppresses gamma oscillations whereas driving these interneurons is sufficient to generate emergent gamma oscillations (Saunders et al. 2013; Sohal et al. 2009). With regard to the pre-stimulus group differences observed in the present study, it is worth noting that optogenetic inhibition of fast-spiking interneurons reduced stimulus-evoked gamma synchrony and also caused an increase in baseline LFP power in the absence of a stimulus (2013).

With regard to the functional significance of the post-stimulus gamma abnormalities in ASD, a recent report using high-density intracortical array recordings demonstrated that synaptic integration within the primary auditory cortex is augmented specifically at the gamma oscillation frequency during passive listening (Rubenstein and Merzenich 2003). That experiment provided strong evidence for a specific, and perhaps obligatory, role for coherent gamma oscillation in listening. The decrease in STG gamma oscillation detected from the scalp using MEG in the immediate post-stimulus period therefore suggests a deficit in synaptic integration in ASD that could not only impact listening but also profoundly impact the downstream integration of auditory information in other areas of cortex.

Thus, as previously suggested (e.g. Rubenstein and Merzenich 2003), post-stimulus gamma abnormalities in ASD likely indicate an abnormal excitatory/inhibitory balance in cortical microcircuits, with this imbalance perhaps indicative of an impairment in information processing during passive listening. Deficits in synaptic integration, perhaps due to the loss of fast-spiking interneurons in ASD, may also explain the elevated ASD pre-stimulus activity observed in the present study (e.g., see Sohal et al. 2009). Neural mechanisms other than GABA and inhibitory interneurons, however, influence oscillatory activity, and additional work is needed to determine which factors are of primary importance in ASD. For

example, white matter diffusion anisotropy in the acoustic radiations of the auditory pathway is associated with M100 latency (Roberts et al. 2009) and it is likely that white matter abnormalities in the acoustic radiations also affect signal-to-noise in primary/secondary auditory areas (especially theta to alpha rhythms).

It is unknown whether an increase in theta to gamma pre-stimulus activity is specific to children with autism or is a more general feature of several neurodevelopmental disorders. For example, although increased pre-stimulus gamma has been reported in schizophrenia (for a review see 2011), it is unknown whether individuals with schizophrenia also show increased pre-stimulus activity in frequencies below gamma. Finally, it is of interest that only gamma-range activity (pre- and post-stimulus) was related to CELF-4 scores. In the left hemisphere a negative association with CELF-4 scores was observed with early post-stimulus evoked gamma activity (i.e., increased post-stimulus activity associated with lower CELF-4 scores). In the right hemisphere a positive association with CELF-4 scores was observed for the pre-stimulus gamma activity (i.e., increased pre-stimulus activity associated with higher CELF-4 scores). Although the above suggests that gamma activity is of particular importance in terms of language abilities in ASD, additional studies are needed to replicate these findings.

A limitation of the present study is that M100 responses were observed less often in the left than in the right hemisphere. For example, for the 500 Hz tone condition, whereas 90 % of the children with ASD had an observable right M100 response, only 63 % had an observable left M100 response. Data from individuals with ASD with perhaps very abnormal auditory activity (i.e., no identifiable M100 response) were thus not included in the hemisphere-specific time-domain and time-frequency analyses. As such, left-hemisphere abnormalities in the present study may be greatly underestimated. Measures of pre-stimulus activity provide support for this claim, as left- but not right-hemisphere pre-stimulus group differences remained after removing variance associated with age.

Given that Rojas et al. (2008) observed ASD and TD group differences in the anterior-posterior position of the left and right M100 generators, a possible limitation of the present study is that although the orientation of the left and right M100 dipoles were individually determined, the left and right M100 STG dipole sources were not individually localized. Localization was not individually performed for the following reasons: (1) M100 source strength is weaker in children than adults (e.g. Paetau et al. 1995); as such, given decreased signal-to-noise, the M100 sources are localized less reliably in young children; (2) left and right STG areas near Heschl's gyrus and the planum temporale are known generators of the M100 response, and a previous study has shown that the use of standard left and right STG sources provides results analogous to those obtained when localizing the sources in each subject (Zvyagintsev et al. 2008), and (3) whereas ASD and TD group differences in the medial to lateral location of the M100 could affect group differences in source strength and thus present a confound when using a standard source model, Rojas et al. (2008) observed only anterior-posterior ASD and TD group differences. However, although unlikely, it is possible that some of the group findings are due to group differences in mis-localization.

Another limitation is that the groups were not matched on gender. Although the pattern of findings generally remained unchanged removing females, future studies with a larger percentage of TD males (or more ASD females) are needed to confirm the present findings. Studies using monaural rather than binaural auditory stimuli are also of interest in order to more specifically examine the contributions of ipsilateral versus contralateral pathways to the observed STG auditory abnormalities.

To summarize, a spectro-temporal profile of ASD was observed, such that auditory STG processes in ASD were characterized by pre-stimulus abnormalities, then early high-frequency abnormalities followed by low-frequency abnormalities. Increased pre-stimulus activity appeared as a 'core' abnormality, with pre-stimulus activity predicting post-stimulus neural abnormalities, group membership, and clinical symptoms (CELF-4 Core Language Index). It is hypothesized that deficits in synaptic integration in the auditory cortex are associated with oscillatory abnormalities in ASD as well as patient symptoms. Increased pre-stimulus activity in ASD likely demonstrates a fundamental signal-to-noise deficit in individuals with ASD, with elevations in oscillatory activity suggesting an inability to maintain an appropriate 'neural tone' and an inability to rapidly return to a resting state prior to the next stimulus.

Supplementary Material

Refer to Web version on PubMed Central for supplementary material.

Acknowledgments

This study was supported in part by NIH grant R01DC008871 (TR), NIH grant R01DC008871-02S1, a NIH grant K08 MH085100 (JCE), Award number P30HD026979 from the Eunice Kennedy Shriver National Institute of Child Health & Human Development of the NIH, and grants from the Nancy Lurie Marks Family Foundation (NLMFF) and Autism Speaks. This research has been funded (in part) by a grant from the Pennsylvania Department of Health. The Pennsylvania Department of Health specifically disclaims responsibility for any analyses, interpretations or conclusions. Dr. Roberts gratefully acknowledges the Oberkircher Family for the Oberkircher Family Chair in Pediatric Radiology at CHOP.

References

- Belforte JE, Zsiros V, Sklar ER, Jiang Z, Yu G, Li Y, et al. Postnatal NMDA receptor ablation in corticolimbic interneurons confers schizophrenia-like phenotypes. *Nature Neuroscience*. 2010; 13(1):76–83. doi:10.1038/nn.2447. [PubMed: 19915563]
- Berg P, Scherg M. A multiple source approach to the correction of eye artifacts. *Electroencephalography and Clinical Neurophysiology*. 1994; 90(3):229–241. [PubMed: 7511504]
- Bibbig A, Traub RD, Whittington MA. Long-range synchronization of gamma and beta oscillations and the plasticity of excitatory and inhibitory synapses: A network model. *Journal of Neurophysiology*. 2002; 88(4):1634–1654. [PubMed: 12364494]
- Canolty RT, Knight RT. The functional role of cross-frequency coupling. *Trends in cognitive sciences*. 2010; 14(11):506–515. [PubMed: 20932795]
- Cantor DS, Thatcher RW, Hrybyk M, Kaye H. Computerized EEG analyses of autistic children. *Journal of Autism and Developmental Disorders*. 1986; 16(2):169–187. [PubMed: 3722118]
- Cardin JA, Carlen M, Meletis K, Knoblich U, Zhang F, Deisseroth K, et al. Driving fast-spiking cells induces gamma rhythm and controls sensory responses. *Nature*. 2009; 459(7247):663–667. doi: 10.1038/nature08002. [PubMed: 19396156]

- Casanova MF, Buxhoeveden DP, Brown C. Clinical and macroscopic correlates of minicolumnar pathology in autism. *Journal of Child Neurology*. 2002; 17(9):692–695. [PubMed: 12503647]
- Cornew L, Roberts TP, Blaskey L, Edgar JC. Resting-state oscillatory activity in autism spectrum disorders. *Journal of Autism and Developmental Disorders*. 2012; 42(9):1884–1894. doi:10.1007/s10803-011-1431-6. [PubMed: 22207057]
- Ehrlichman RS, Gandal MJ, Maxwell CR, Lazarewicz MT, Finkel LH, Contreras D, et al. N-methyl-d-aspartic acid receptor antagonist-induced frequency oscillations in mice recreate pattern of electrophysiological deficits in schizophrenia. *Neuroscience*. 2009; 158(2):705–712. [PubMed: 19015010]
- Fatemi SH, Reutiman TJ, Folsom TD, Thuras PD. GABA(A) receptor downregulation in brains of subjects with autism. *Journal of Autism and Developmental Disorders*. 2009; 39(2):223–230. doi: 10.1007/s10803-008-0646-7. [PubMed: 18821008]
- Gage NM, Siegel B, Callen M, Roberts TP. Cortical sound processing in children with autism disorder: An MEG investigation. *Neuroreport*. 2003; 14(16):2047–2051. [PubMed: 14600495]
- Hakami T, Jones NC, Tolmacheva EA, Gaudias J, Chaumont J, Salzberg M, et al. NMDA receptor hypofunction leads to generalized and persistent aberrant gamma oscillations independent of hyperlocomotion and the state of consciousness. *PLoS ONE*. 2009; 4(8):e6755. doi:10.1371/journal.pone.0006755. [PubMed: 19707548]
- Hoehstetter K, Bornfleth H, Weckesser D, Ille N, Berg P, Scherg M. BESA source coherence: A new method to study cortical oscillatory coupling. *Brain Topography*. 2004; 16(4):233–238. [PubMed: 15379219]
- Jackson ME, Homayoun H, Moghaddam B. NMDA receptor hypofunction produces concomitant firing rate potentiation and burst activity reduction in the prefrontal cortex. *Proceedings of the National Academy of Sciences of the United States of America*. 2004; 101(22):8467–8472. [PubMed: 15159546]
- Lachaux JP, Rodriguez E, Martinerie J, Varela FJ. Measuring phase synchrony in brain signals. *Human Brain Mapping*. 1999; 8(4):194–208. [PubMed: 10619414]
- Lakatos P, Szilagyi N, Pincze Z, Rajkai C, Ulbert I, Karmos G. Attention and arousal related modulation of spontaneous gamma-activity in the auditory cortex of the cat. *Brain Research. Cognitive Brain Research*. 2004; 19(1):1–9. doi:10.1016/j.cogbrainres.2003.10.023. [PubMed: 14972353]
- Lazarewicz MT, Ehrlichman RS, Maxwell CR, Gandal MJ, Finkel LH, Siegel SJ. Ketamine modulates theta and gamma oscillations. *Journal of Cognitive Neuroscience*. 2010; 22(7):1452–1464. doi: 10.1162/jocn.2009.21305. [PubMed: 19583475]
- Leung LW. Spectral analysis of hippocampal EEG in the freely moving rat: Effects of centrally active drugs and relations to evoked potentials. *Electroencephalography and Clinical Neurophysiology*. 1985; 60(1):65–77. [PubMed: 2578356]
- Lins OG, Picton TW, Berg P, Scherg M. Ocular artifacts in recording EEGs and event-related potentials. II: Source dipoles and source components. *Brain Topography*. 1993; 6(1):65–78. [PubMed: 8260328]
- Ma J, Leung LS. Relation between hippocampal gamma waves and behavioral disturbances induced by phencyclidine and methamphetamine. *Behavioural Brain Research*. 2000; 111(1–2):1–11. [PubMed: 10840127]
- Ma J, Leung LS. The supramammillo-septal-hippocampal pathway mediates sensorimotor gating impairment and hyperlocomotion induced by MK-801 and ketamine in rats. *Psychopharmacology (Berl)*. 2007; 191(4):961–974. [PubMed: 17219218]
- Murias M, Webb SJ, Greenson J, Dawson G. Resting state cortical connectivity reflected in EEG coherence in individuals with autism. *Biological Psychiatry*. 2007; 62(3):270–273. doi:10.1016/j.biopsych.2006.11.012. [PubMed: 17336944]
- Oram Cardy JE. Auditory evoked fields predict language ability and impairment in children. *International Journal of Psychophysiology*. 2008; 68(2):170–175. [PubMed: 18304666]
- Orehkova EV, Stroganova TA, Nygren G, Tsetlin MM, Posikera IN, Gillberg C, et al. Excess of high frequency electroencephalogram oscillations in boys with autism. *Biological Psychiatry*. 2007; 62(9):1022–1029. [PubMed: 17543897]

- Paetau R, Ahonen A, Salonen O, Sams M. Auditory evoked magnetic fields to tones and pseudowords in healthy children and adults. *Journal of Clinical Neurophysiology*. 1995; 12(2):177–185. [PubMed: 7797632]
- Papp N, Ktonas P. Critical evaluation of complex demodulation techniques for the quantification of bioelectrical activity. *Biomedical Sciences Instrumentation*. 1977; 13:135–145. [PubMed: 871500]
- Pinault D. N-methyl d-aspartate receptor antagonists ketamine and MK-801 induce wake-related aberrant gamma oscillations in the rat neocortex. *Biological Psychiatry*. 2008; 63(8):730–735. [PubMed: 18022604]
- Roberts TP, Cannon KM, Tavabi K, Blaskey L, Khan SY, Monroe JF, et al. Auditory magnetic mismatch field latency: A biomarker for language impairment in Autism. *Biological Psychiatry*. 2011; 70(3):263–269. doi:10.1016/j.biopsych.2011.01.015. [PubMed: 21392733]
- Roberts TP, Khan SY, Blaskey L, Dell J, Levy SE, Zarnow DM, et al. Developmental correlation of diffusion anisotropy with auditory-evoked response. *Neuroreport*. 2009; 20(18):1586–1591. doi: 10.1097/WNR.0b013e3283306854. [PubMed: 19898261]
- Roberts TP, Khan SY, Rey M, Monroe JF, Cannon K, Blaskey L, et al. MEG detection of delayed auditory evoked responses in autism spectrum disorders: Towards an imaging biomarker for autism. *Autism Research*. 2010; 3(1):8–18. doi:10.1002/aur.111. [PubMed: 20063319]
- Roberts TP, Schmidt GL, Egeth M, Blaskey L, Rey MM, Edgar JC, et al. Electrophysiological signatures: Magnetoencephalographic studies of the neural correlates of language impairment in autism spectrum disorders. *International Journal of Psychophysiology*. 2008; 68(2):149–160. [PubMed: 18336941]
- Rojas DC, Maharajh K, Teale P, Rogers SJ. Reduced neural synchronization of gamma-band MEG oscillations in first-degree relatives of children with autism. *BMC Psychiatry*. 2008; 8:66. [PubMed: 18673566]
- Rubenstein JL, Merzenich MM. Model of autism: Increased ratio of excitation/inhibition in key neural systems. *Genes Brain Behavior*. 2003; 2(5):255–267.
- Santana N, Troyano-Rodriguez E, Mengod G, Celada P, Artigas F. Activation of thalamocortical networks by the N-methyl-D-aspartate receptor antagonist phencyclidine: reversal by clozapine. *Biological Psychiatry*. 2011; 69(10):918–927. doi:10.1016/j.biopsych.2010.10.030. [PubMed: 21251645]
- Saunders JA, Gandal MJ, Roberts TP, Siegel SJ. NMDA antagonist MK801 recreates auditory electrophysiology disruption present in autism and other neurodevelopmental disorders. *Behavioural Brain Research*. 2012; 234(2):233–237. [PubMed: 22771812]
- Saunders JA, Tatar-Leitman VM, Suh J, Billingslea EN, Roberts TP, Siegel SJ. Knockout of NMDA receptors in parvalbumin interneurons recreates autism-like phenotypes. *Autism Research*. 2013; 6(2):69–77. doi:10.1002/aur.1264. [PubMed: 23441094]
- Scherg, M. Fundamentals of dipole source potential analysis, in *Auditory evoked magnetic fields and electric potentials*. In: Gandori, MHGLR., editor. *Advances in audiology*. Karger; Basel, Switzerland: 1990. p. 40-69.
- Scherg M, Berg P. New concepts of brain source imaging and localization. *Electroencephalography and Clinical Neurophysiology. Supplement*. 1996; 46:127–137. [PubMed: 9059786]
- Scherg M, Ebersole JS. Brain source imaging of focal and multifocal epileptiform EEG activity. *Neurophysiologie Clinique*. 1994; 24(1):51–60. [PubMed: 8121338]
- Scherg M, Ille N, Bornfleth H, Berg P. Advanced tools for digital EEG review: Virtual source montages, whole-head mapping, correlation, and phase analysis. *Journal of Clinical Neurophysiology*. 2002; 19(2):91–112. [PubMed: 11997721]
- Scherg M, von Cramon D. A new interpretation of the generators of BAEP waves I-V: Results of a spatio-temporal dipole model. *Electroencephalography and Clinical Neurophysiology*. 1985; 62(4):290–299. [PubMed: 2408875]
- Sohal VS, Zhang F, Yizhar O, Deisseroth K. Parvalbumin neurons and gamma rhythms enhance cortical circuit performance. *Nature*. 2009; 459(7247):698–702. doi:10.1038/nature07991. [PubMed: 19396159]

- Tamas G, Buhl EH, Lorincz A, Somogyi P. Proximally targeted GABAergic synapses and gap junctions synchronize cortical interneurons. *Nature Neuroscience*. 2000; 3(4):366–371. doi: 10.1038/73936. [PubMed: 10725926]
- Uhlhaas PJ, Singer W. What do disturbances in neural synchrony tell us about autism? *Biological Psychiatry*. 2007; 62(3):190–191. [PubMed: 17631116]
- Wechsler, D. Wechsler intelligence scale for children. Vol. 3. The Psychological Corporation; San Antonio, TX: 2003.
- Whittington MA, Traub RD, Jefferys JG. Synchronized oscillations in interneuron networks driven by metabotropic glutamate receptor activation. *Nature*. 1995; 373(6515):612–615. [PubMed: 7854418]
- Whittington MA, Traub RD, Kopell N, Ermentrout B, Buhl EH. Inhibition-based rhythms: Experimental and mathematical observations on network dynamics. *International Journal of Psychophysiology*. 2000; 38(3):315–336. [PubMed: 11102670]
- Wilson TW, Rojas DC, Reite ML, Teale PD, Rogers SJ. Children and adolescents with autism exhibit reduced MEG steady-state gamma responses. *Biological Psychiatry*. 2007; 62(3):192–197. [PubMed: 16950225]
- Zvyagintsev M, Thonnessen H, Dammers J, Boers F, Mathiak K. An automatic procedure for the analysis of electric and magnetic mismatch negativity based on anatomical brain mapping. *Journal of Neuroscience Methods*. 2008; 168(2):325–333. [PubMed: 18093661]

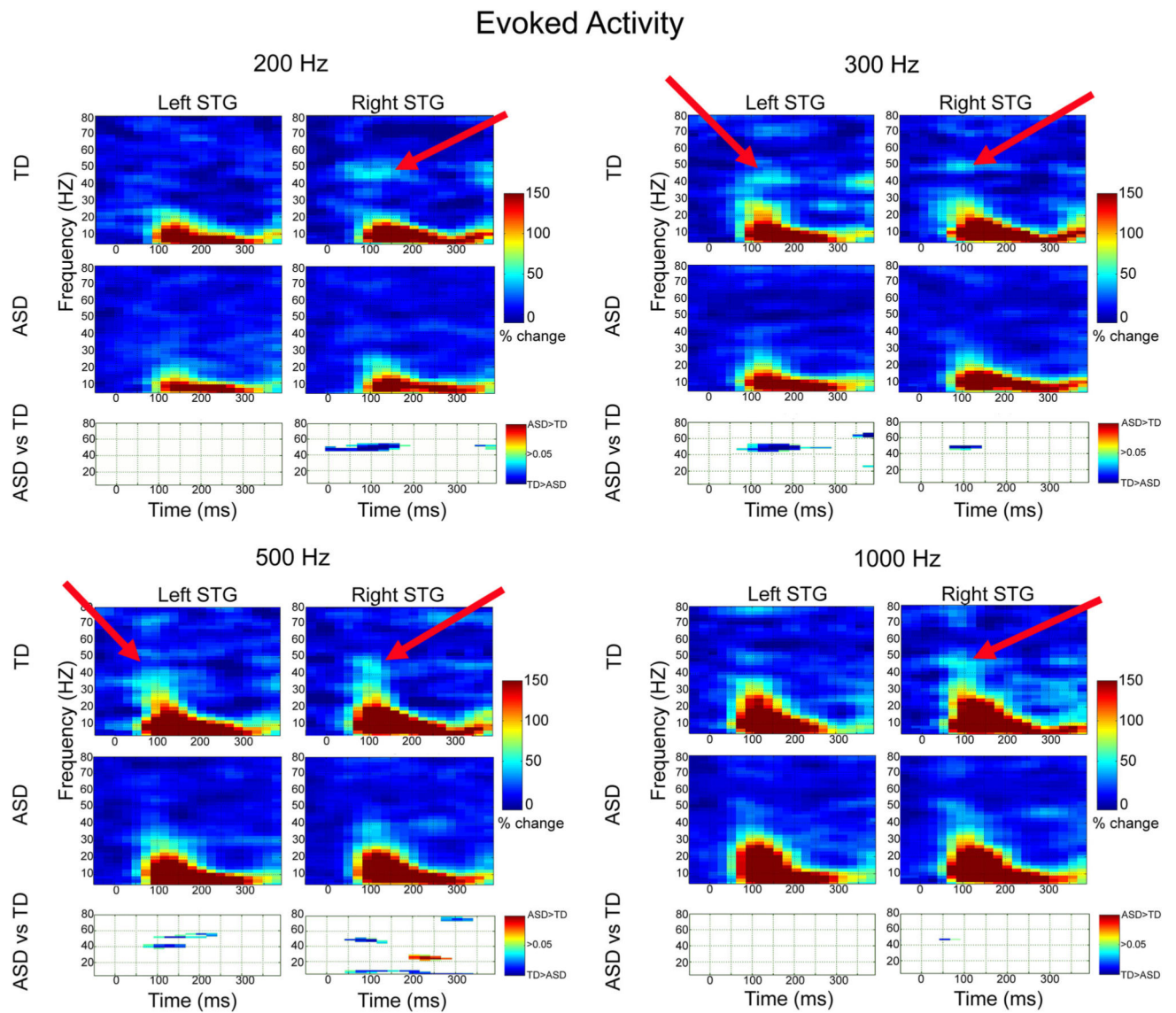


Fig. 1. Evoked activity and familywise-corrected p value plots comparing TD and ASD for each frequency. TD > ASD differences are shown in *blue*, ASD > TD differences in *red*. *Red arrows* show examples of where greater evoked gamma activity was observed in TD than ASD

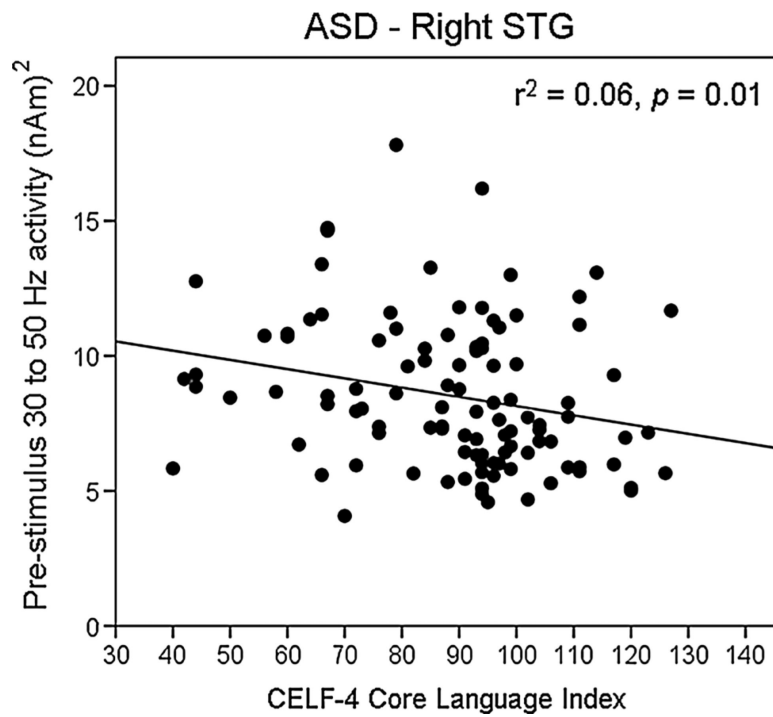


Fig. 3. Scatterplot of CELF-4 Core Language Index scores (*x axis*) and right STG pre-stimulus gamma activity (*y axis*; 30–50 Hz) in individuals with ASD. In ASD, lower CELF-4 scores were associated with increased right-hemisphere pre-stimulus gamma activity

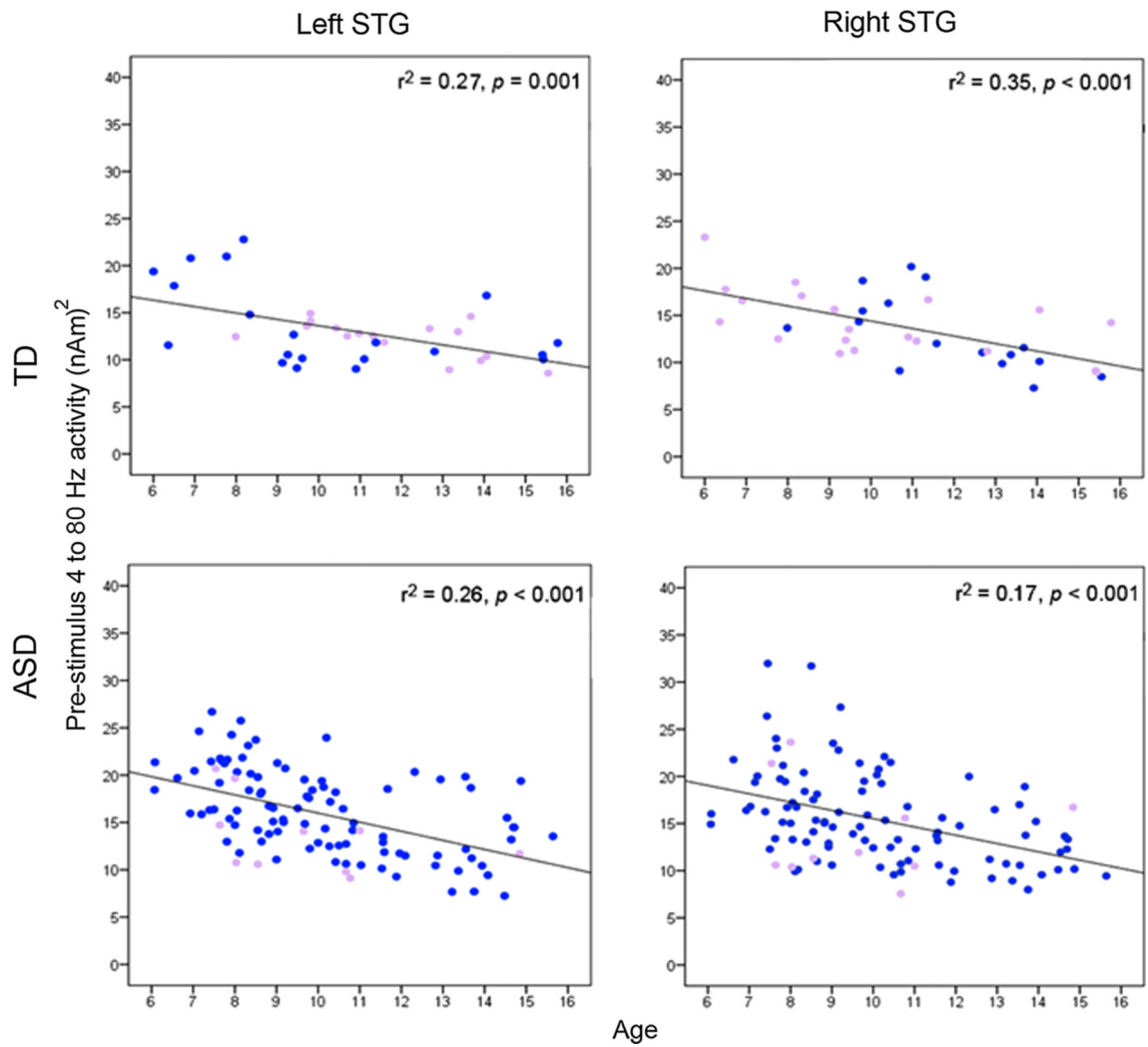


Fig. 4. Scatterplots of age (*x axis*) and pre-stimulus total power (average of 4–80 Hz activity; *y axis*). In TD (*top row*) and ASD (*bottom row*), increased pre-stimulus activity predicted a younger age. Males are shown in *blue* and females in *purple*

Table 1

Pre-stimulus group differences were assessed after averaging the trials for all tones (approximately 420 trials)

Frequency band	TD left STG	ASD left STG	<i>p</i> value	TD right STG	ASD right STG	<i>p</i> value
Theta (4–8 Hz)	45.84 (13.39)	55.52 (17.16)	<i>p</i> = 0.003	41.52 (10.14)	49.46 (13.45)	<i>p</i> = 0.002
Alpha (8–12 Hz)	30.38 (9.31)	35.47 (11.50)	<i>p</i> = 0.02	27.17 (6.75)	31.41 (9.093)	<i>p</i> = 0.01
Beta (13–20 Hz)	19.12 (5.00)	22.94 (6.91)	<i>p</i> = 0.003	18.07 (4.38)	20.72 (5.44)	<i>p</i> = 0.01
Low Gamma (20–56)	7.84 (1.58)	9.52 (2.39)	<i>p</i> < 0.001	8.06 (1.70)	9.07 (2.33)	<i>p</i> = 0.02
High Gamma (64–80 Hz)	4.80 (1.17)	6.13 (1.76)	<i>p</i> < 0.001	5.80 (1.85)	6.13 (2.11)	<i>p</i> = 0.42

Group means (SD) and *p* values are reported for the left and right STG for theta, alpha, beta, low gamma, and high gamma

Author Manuscript

Author Manuscript

Author Manuscript

Author Manuscript